

# SLP-65 Phosphorylation Dynamics Reveals a Functional Basis for Signal Integration by Receptor-proximal Adaptor Proteins\*<sup>§</sup>

Thomas Oellerich<sup>‡§</sup>, Mads Grønborg<sup>¶\*\*</sup>, Konstantin Neumann<sup>‡</sup>, He-Hsuan Hsiao<sup>¶</sup>, Henning Urlaub<sup>¶‡‡</sup>, and Jürgen Wienands<sup>‡§§</sup>

Understanding intracellular signal transduction by cell surface receptors requires information about the precise order of relevant modifications on the early transducer elements. Here we introduce the B cell line DT40 and its genetically engineered variants as a model system to determine and functionally characterize post-translational protein modifications in general. This is accomplished by a customized strategy that combines mass spectrometric analyses of protein modifications with subsequent mutational studies. When applied to the B cell receptor (BCR)-proximal effector SLP-65, this approach uncovered a differential and highly dynamic engagement of numerous newly identified phospho-acceptor sites. Some of them serve as kinase substrates in resting cells and undergo rapid dephosphorylation upon BCR ligation. Stimulation-induced phosphorylation of SLP-65 can be early and transient, or early and sustained, or late. Functional elucidation of conspicuous phosphorylation at serine 170 in SLP-65 revealed a BCR-distal checkpoint for some but not all possible B cell responses. Our data show that SLP-65 phosphorylation acts upstream for signal initiation and also downstream during selective processing of the BCR signal. Such a phenomenon defines a receptor-specific signal integrator. *Molecular & Cellular Proteomics* 8:1738–1750, 2009.

Cell surface receptors regulate multiple and overlapping sets of intracellular signaling proteins. These effector molecules can be structurally organized into distinct signaling cascades, which act in concert to coordinate precise cellular responses following receptor engagement (1, 2). Immediate early reactions include reorganization of the actin cytoskeleton associated with changes in cell morphology and migration (3–5). Late reactions such as proliferation and differentiation require altered gene transcription (6–8). To limit cellular responses and to prevent neoplastic transformation, activated

receptors also initiate inhibitory feedback loops in an autonomous manner (9).

In most cases, cell surface receptors do not couple directly to distinct signal chains. Instead they employ receptor-proximal adaptor proteins, which are devoid of enzymatic activity but become inducibly modified by phosphorylation (1, 10). This enables them to act as a transducer platform to collect and integrate incoming signals. As a consequence, intracellular signal transduction is not linear, *i.e.* one receptor-specific adaptor can simultaneously control different positive as well as negative signaling cascades. The molecular basis for the pleiotropic yet specific processing of signals is still poorly understood.

The multimeric antigen receptors on B and T lymphocytes utilize adaptors called SLP<sup>1</sup> (Src homology (SH) 2 domain-containing leukocyte proteins) (11). B cells express the 65 kDa family member SLP-65 (12), (also named BLNK (13) or BASH (14)) encompassing an N-terminal basic effector domain, various tyrosine phosphorylation sites, several consensus binding motifs for SH3 domains, and a C-terminal SH2 domain. Biochemical and genetic studies have established the mandatory role of SLP-65 for antigen-induced B cell activation and the subsequent initiation of immune effector functions (15). Moreover, the antigen-independent generation of B cells in the bone marrow also requires SLP-65 expression. In the absence of SLP-65, B cell development is severely compromised in mouse and man (16–19). The dual role of SLP-65 for the development and activation of B cells demonstrates a remarkable plasticity of the BCR signaling machinery (20). The underlying molecular details, which allow BCR signal modulation in a differentiation stage-specific manner, are unknown.

A key event for the activation of peripheral B cells is the BCR-induced tyrosine phosphorylation of SLP-65. This enables SLP-65 to nucleate the formation of a multiprotein complex by recruiting several SH2 domain-containing effector

From the <sup>‡</sup>Institute of Cellular and Molecular Immunology, Georg August University of Göttingen, Humboldtallee 34, 37073 Göttingen, Germany and <sup>¶</sup>Bioanalytical Mass Spectrometry Group and <sup>||</sup>Department of Neurobiology, Max Planck Institute for Biophysical Chemistry, Am Fassberg 11, 37077 Göttingen, Germany

Received, December 10, 2008, and in revised form, April 9, 2009  
Published, MCP Papers in Press, April 16, 2009, DOI 10.1074/mcp.M800567-MCP200

<sup>1</sup> The abbreviations used are: SLP, Src homology 2 domain-containing leukocyte proteins; SH, Src homology; BCR, B cell receptor; PLC, phospholipase C; MAP, mitogen-activated protein; Erk, extracellular signal-regulated kinase; JNK, c-Jun NH<sub>2</sub>-terminal kinase; AP1, activator protein-1; MS, mass spectrometry; SILAC, stable isotope labeling by amino acids in cell culture; GFP, green fluorescent protein; wt, wild-type; ACN, acetonitrile; EGFP, enhanced green fluorescent protein; 1D, one-dimensional; FCS, fetal calf serum.

proteins such as phospholipase (PLC)- $\gamma$ 2 and Bruton's tyrosine kinase (21). SLP-65 not only assembles this signalosome but is also critical for its stimulation-induced translocation from the cytosol to the plasma membrane (22, 23). Assembly and membrane targeting of this complex are both requisites for PLC- $\gamma$ 2 to hydrolyze membrane phospholipids resulting in the generation of diacylglycerol and inositol triphosphate, which in turn induces the release and entry of  $\text{Ca}^{2+}$  ions from intra- and extracellular sources, respectively (24–26). These second messengers are upstream regulators of several B cell activation cascades. They trigger nuclear translocation of cytosolic transcription factors such as NF- $\kappa$ B or nuclear factor of activated T-cells (NFAT) (26) and activation of serine/threonine kinases such mitogen-activated protein (MAP) kinases. BCR stimulation can potentially activate all three MAP kinase family members, *i.e.* extracellular signal-regulated kinase (Erk), c-Jun NH<sub>2</sub>-terminal kinase (JNK), and p38 (27). A prominent MAP kinase activation target is the transcription factor activator protein-1 (AP1), which is a heterodimer of c-Fos and c-Jun proto-oncoproteins (28). Hence, tyrosine phosphorylation of SLP-65 provides a single trigger for a series of canonical and lymphocyte-specific signaling pathways.

More complex levels of regulation must however exist to fulfill the different BCR signaling requirements during the development of B cells on the one hand and their activation upon antigen encounter in secondary lymph organs on the other hand. Indeed, recent studies showed that SLP-65 is capable of regulating MAP kinase activity in an inositol triphosphate/diacylglycerol-independent manner (25, 29). These data suggest that phosphotyrosine-dependent and phosphotyrosine-independent processes cooperate to modulate SLP-65 signal output for early and late activation events. A likely mode of signal adjustment is phosphorylation of SLP-65 on serine and threonine residues as this has been reported to regulate adaptor protein function in several signaling pathways including T cell receptor-mediated signaling (30). Moreover, the majority of putative phospho-acceptor sites within SLP-65 are serine and threonine residues, but their role in BCR signaling has not yet been explored. A molecular understanding of the complete SLP-65 network thus requires a comprehensive and kinetic analysis of its phosphorylation states in resting and stimulated B cells by functional proteomic approaches.

The qualitative and quantitative analyses of protein phosphorylation cycles has been greatly improved by the introduction of enrichment techniques for phosphorylated peptides such as titanium dioxide ( $\text{TiO}_2$ )-based purification, which combined with subsequent state-of-the-art mass spectrometry (MS) have paved the way for rapid and reliable phosphoproteome analyses (31, 32). The additional implementation of stable isotope labeling by amino acids in cell culture (SILAC) allowed a more detailed view on differential phosphorylation events and their time-dependent dynamics (33, 34). However, the functional phosphoproteomic analysis of a given effector

protein, such as SLP-65, is hampered by two obstacles. First, signaling molecules, especially eukaryotic proteins, are often difficult to enrich because of limited physiological sources. Second, experimental systems to assess the functional relevance of post-translational protein modifications are almost lacking.

We have now employed the DT40 B cell reconstitution system (35) to purify wild-type SLP-65 in large amounts, to subject it to qualitative and quantitative MS-based phosphoproteomic analysis and lastly, to test *in vivo* the importance of individual phosphorylation sites for distinct signaling pathways by site-directed mutagenesis. This comprehensive approach has identified SLP-65 as one of the most phosphorylated proteins known so far. It has also revealed an unexpected complexity in the phosphorylation kinetics of distinct phospho-acceptor sites, which together with a functional crosstalk between tyrosine and serine/threonine phosphorylation events fine-tunes MAP kinase and AP1 activation. Our data help to explain how SLP-65 can act as a BCR-proximal master activator for many signaling pathways while retaining the possibility of signal modulation. Furthermore, these results demonstrate that the DT40 system is a useful tool for combined proteomic and functional analyses.

#### EXPERIMENTAL PROCEDURES

**DT40 Cell Culture, Antibodies, and Reagents**—Wild-type chicken DT40 cells and the SLP-65-deficient mutant (kindly provided by T. Kurosaki, Yokohama, Japan) were cultured in RPMI 1640 supplemented with 10% fetal calf serum, 1% chicken serum, 3 mM L-glutamine, and antibiotics. SLP-65-deficient DT40 cells are described by Ishiai *et al.* (25). BCR stimulation of the cells was performed with 2  $\mu\text{g}/\text{ml}$  anti-chicken IgM (M4, Southern Biotechnology, BioMol, Hamburg, Germany). For cell lysis 1% Nonidet P-40 buffer containing 50 mM Tris/HCl, pH 7.8, 150 mM NaCl, 0.5 mM EDTA, 2 mM  $\text{Na}_3\text{VO}_4$ , 1 mM NaF, 10% glycerol, and protease inhibitors P2714 (Sigma-Aldrich) was used. SLP-65 was immunoprecipitated from lysates of  $2 \times 10^7$  cells with either anti-chicken SLP-65 (kindly provided by T. Kurosaki) or anti-GFP (Roche) antibodies immobilized by protein A/G-Sepharose (Pierce) according to the manufacturer's instructions. Antibodies for immunoblotting are specific for phosphotyrosine (4G10; BioMol), Erk (BD Biosciences), p38 (Cell Signaling Technology), or actin (Sigma-Aldrich). Phospho-specific antibodies recognizing phospho-Erk, phospho-p38, phospho-JNK, or phospho-14-3-3-binding sites were purchased from Cell Signaling Technology.

**Expression Constructs, Transfections, and Retroviral Transductions**—The cDNA encoding chicken SLP-65 with an N-terminal One-STRIP-Tag (Iba BioTAGnology, Göttingen, Germany) was cloned into pAbes-puro (kindly provided by M. Reth, Freiburg, Germany). The resulting expression plasmid was introduced into SLP-65-deficient DT40 B cells by electroporation (300 V, 975  $\mu\text{F}$ ). Transfectants were selected in the presence of 1  $\mu\text{g}/\text{ml}$  puromycin, and protein expression was confirmed by immunoblot analysis. The cDNA encoding N-terminally EGFP-tagged chSLP-65 was inserted into pCRII-Topo vector. Site-directed mutagenesis (QuikChange) was used to generate the S170A and S173A mutants of SLP-65. cDNAs encoding EGFP fusion proteins encompassing either wild-type or mutant SLP-65 (EGFP-SLP-65-wt, EGFP-SLP-65-S170A, or -S173A, respectively) were inserted into pMSCV, and SLP-65-deficient B cells were retrovirally transduced as described (36).

**Affinity Purification of Chicken SLP-65 upon SILAC**—SILAC was performed by culturing DT40 cells in RPMI 1640 medium devoid of arginine and lysine (Pierce) supplemented with 10% dialyzed FCS (Invitrogen), 1 mM pyruvate, and 4 mM glutamine. “Heavy”, “intermediate”, and “light” medium were prepared by adding 0.115 mM  $^{13}\text{C}_6$  $^{15}\text{N}_4$  L-arginine and 0.275 mM  $^{13}\text{C}_6$  $^{15}\text{N}_2$  L-lysine (Sigma Isotec), or equimolar levels of  $^{13}\text{C}_6$  $^{14}\text{N}_4$  L-arginine and L-lysine-4,4,5,5-D4 (Cambridge Isotopes), or the corresponding non-labeled amino acids (Sigma-Aldrich), respectively. For affinity purification of One-StrEP-tagged chSLP-65 labeled with either heavy, intermediate, or light isotopes,  $10^8$  DT40 B cell transfectants from the respective cultures were left untreated or BCR-stimulated and lysed. Following determination of protein concentrations (37) lysates were pooled at a 1:1:1 ratio and incubated with 200  $\mu\text{l}$  of Strep-Tactin Superflow matrix (Iba BioTAGnology) for 1 h at 4 °C. The immobilized chSLP-65 was eluted at room temperature with 500  $\mu\text{l}$  of D-Desthiobiotin elution buffer (Iba BioTAGnology) and concentrated with ultrafiltration spin columns (Sartorius, Göttingen, Germany).

**TiO<sub>2</sub> Enrichment Procedure**—Phosphopeptides were enriched by TiO<sub>2</sub> chromatography (GL Sciences Inc., Tokyo, Japan) as described by Larsen *et al.* (32). In brief, aliquots of peptides were dissolved with 20  $\mu\text{l}$  of 200-mg 2,5-dihydroxybenzoic acid (DHB; Sigma-Aldrich) in 80% acetonitrile (ACN), 5% trifluoroacetic acid and loaded onto a TiO<sub>2</sub> column. The column was washed three times with 20  $\mu\text{l}$  of 200-mg DHB in 80% ACN, 5% trifluoroacetic acid and five times with 20  $\mu\text{l}$  of 80% ACN, 5% trifluoroacetic acid. The column was then incubated three times with 20  $\mu\text{l}$  of 0.3 normal (N) NH<sub>4</sub>OH, pH  $\geq$  10.5, and subsequently bound peptides were eluted and afterward evaporated with a SpeedVac for further MS analysis.

**NanoLC-ESI Mass Spectrometry Analysis and Mascot Database Searching**—Enriched tryptic peptides were first loaded at a flow rate of 10  $\mu\text{l}/\text{min}$  onto a C18 trap column packed in-house (1.5 cm, 360- $\mu\text{m}$  outer diameter, 150- $\mu\text{m}$  inner diameter, Nucleosil 100-5 C18; MACHEREY-NAGEL, GmbH & Co. KG). The peptides retained were then eluted and separated on an analytical C18 capillary column (30 cm, 360- $\mu\text{m}$  outer diameter, 75  $\mu\text{m}$ -inner diameter, Nucleosil 100-5 C18) at a flow rate of 300 nL/min, with a gradient from 7.5 to 37.5% ACN in 0.1% (v/v) formic acid for 60 min using an Agilent 1100 nano-flow LC system (Agilent Technologies, Palo Alto, CA), coupling with Ultima™ API-Q-TOF mass spectrometer (Waters/Micromass, Milford, MA) or LTQ-Orbitrap XL hybrid mass spectrometer (Thermo Electron, Bremen, Germany). The API-Q-TOF was operated in data-dependent acquisition mode. Briefly, 1 s survey scans were run over the mass range  $m/z$  350 to 1600. A maximum of three concurrent MS/MS acquisitions were triggered for doubly, triply, and quadruply charged precursors detected at intensities above 15 counts; after 3 s of acquisition, the system switched back to survey scan mode. A Q-TOF peaklist file was generated by MassLynx 4.0 SP4. All spectra were searched by using MASCOT v2.2.04 against the Swiss-Prot database (20080701/39069 entries) limited to chicken with the following criteria: peptide mass tolerance, 50 ppm; MS/MS ion mass tolerance, 0.25 Da; number of missed cleavages allowed, up to three; the variable modifications considered were phosphorylation of serine, threonine and tyrosine, methionine oxidation, and cysteine carboxyamidomethylation. The LTQ-Orbitrap was operated in the data-dependent mode. Briefly, survey full scan MS spectra were acquired in the orbitrap ( $m/z$  350–1600) with the resolution set to 30,000 at  $m/z$  400 and automatic gain control target at  $10^6$ . The five most intense ions were sequentially isolated for collision-induced decay MS/MS fragmentation and detection in the linear ion trap with previously selected ions dynamically excluded for 90 s. Ions with single and unrecognized charge states were also excluded. To improve the fragmentation spectra of the phosphopeptides, “multistage activation” corresponding to a neutral loss of phosphoric acid from doubly

and triply charged precursor ions was enabled in all MS/MS events. All the measurements in the orbitrap were performed with the lock mass option (lock mass:  $m/z$  445,120025) for internal calibration. Orbitrap DTA files were generated by BioWorks version 3.3.1 SP1 and were merged and converted to MASCOT generic format files. All spectra were searched using MASCOT v2.2.04 against the Swiss-Prot database limited to chicken with the following criteria: peptide mass tolerance, 10 ppm; MS/MS ion mass tolerance, 0.8 Da; number of missed cleavages allowed, up to three. The variable modifications considered were phosphorylation of serine, threonine and tyrosine, methionine oxidation, and cysteine carboxyamidomethylation. All phosphorylated sites were examined manually by the presence of a mass difference of 69 Da between fragment ions for phosphoserine and a difference of 83 Da for phosphothreonine (see supplemental data). Quantification of phosphopeptides was performed by using MSQuant. Preselected peptides with a score greater 10 were validated. For quantification the combined peak intensities of each phosphorylated peptide were compared. All phosphorylated sites were examined manually (see supplemental data).

**BCR-induced Ca<sup>2+</sup> Mobilization and Activation of Luciferase Reporter**—For recording intracellular Ca<sup>2+</sup> concentrations,  $10^6$  DT40 cells were loaded with the ratiometric Ca<sup>2+</sup> chelator Indo-1 AM (Molecular Probes, BioMol) at a concentration of 1  $\mu\text{M}$  in 1-ml RPMI 1640 10% FCS for 30 min at 30 °C. Subsequently, cells were washed twice with and resuspended in a Krebs Ringer solution composed of 10 mM HEPES (pH 7.0), 140 mM NaCl, 4 mM KCl, 1 mM MgCl<sub>2</sub>, 1 mM CaCl<sub>2</sub>, and 10 mM glucose. After monitoring basal Ca<sup>2+</sup> concentrations, cells were BCR-stimulated, and the ratio of Ca<sup>2+</sup>-bound to Ca<sup>2+</sup>-unbound Indo-1 (Indo-1 violet/Indo-1 blue) was monitored on an LSR II cytometer (Becton Dickinson) at wavelengths 440 and 510 nm. For analysis of BCR-induced AP1 activation,  $2 \times 10^7$  DT40 cells were cotransfected by electroporation (300 V, 975  $\mu\text{F}$ ) with 10  $\mu\text{g}$  of a  $\beta$ -galactosidase expression plasmid (pCMV $\beta$ ; BD Biosciences - Clontech) and 20  $\mu\text{g}$  of an AP1-driven luciferase reporter gene plasmid (3  $\times$  TRE/tk) as described in Ref. 38. Transfectants were cultured 48 h and subsequently starved for 12 h in RPMI 1640 1% FCS. Luciferase and  $\beta$ -galactosidase activities were assayed and standardized as described by Brummer *et al.* (39) for resting DT40 B cells and cells stimulated through their BCR for 6 h with M4 monoclonal antibody at a concentration of 2  $\mu\text{g}/\text{ml}$ . Where indicated, cells were pretreated one hour prior to BCR stimulation with SB202190 or SP600125 (Biomol) to inhibit p38 or JNK, respectively (29).

## RESULTS

**Tagged SLP-65 Restores BCR Signaling in SLP-65-deficient DT40 B Cells**—The chicken B cell line DT40 is highly susceptible to homologous recombination of gene fragments (40). Hence, DT40 cells have been widely used for targeted disruption of genes including the gene encoding SLP-65 (25). We set out to take advantage of this system to establish a basis for allowing easy acquisition of proteomic data sets including those on post-translational protein modifications and their subsequent functional evaluation by genetic means.

We first reconstituted SLP-65-deficient DT40 cells with wild-type avian SLP-65 harboring an N-terminal One-StrEP-Tag (IBA BioTAGnology). Expression of tagged SLP-65 was controlled by anti-SLP-65 immunoblotting of cleared cellular lysates (Fig. 1A). The attachment of the N-terminal peptide tag was aimed at facilitating the affinity purification of SLP-65 via a biotin-based matrix. The modification however made it nec-

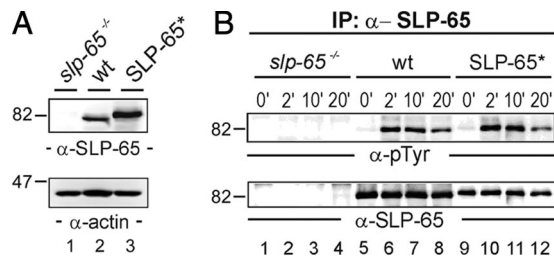


**FIG. 1. Functional reconstitution of BCR signaling by peptide-tagged SLP-65.** *A*, cleared cellular lysates of SLP-65-deficient DT40 B cell mutants (*slp-65*<sup>-/-</sup>; lane 1), wild-type DT40 cells (*wt*; lane 2), and reconstituted DT40 mutants expressing a SLP-65 version harboring a One-STrEP peptide tag at the N-terminal end (*SLP-65\**; lane 3) were subjected to immunoblot analysis with antibodies against chicken SLP-65 (*upper panel*). Equal protein loading was ensured by anti-actin immunoblotting (*lower panel*). *B*, cells described in *A* were left untreated (0 min; lanes 1, 5, and 9) or stimulated through their BCR for 2 (lanes 2, 6, and 10), 10 (lanes 3, 7, and 11), and 20 min (lanes 4, 8, and 12). From the cleared cellular lysates, SLP-65 proteins were purified by anti-SLP-65 immunoprecipitation and analyzed by anti-phosphotyrosine or anti-chicken SLP-65 immunoblotting (*upper and lower panel*, respectively).

essary to test the functionality of this SLP-65 version. As shown in Fig. 1*B*, following BCR activation tagged SLP-65 was phosphorylated on tyrosine residues with the same kinetics as endogenously expressed SLP-65. The BCR-induced Ca<sup>2+</sup> mobilization profiles of wild-type cells and SLP-65-reconstituted DT40 cells overlapped (data not shown). Hence the presence of the N-terminal tag does not impair coupling of the activated BCR to SLP-65.

**SLP-65 Is Post-translationally Modified with 41 Phosphoryl Groups**—For qualitative identification of SLP-65 phosphorylation sites, we affinity-purified SLP-65 from DT40 cells that were either left untreated or were stimulated through their IgM-BCR for 2 or 20 min. Following size separation by 1D-PAGE, SLP-65 was in-gel-digested with endoproteases trypsin and/or chymotrypsin. Resulting phosphopeptide products were enriched by TiO<sub>2</sub> microcolumns and subjected to LC-MS/MS using a Q-ToF or an orbitrap mass spectrometer. The Q-ToF mass spectrometer has the advantage that the resulting fragment spectra are of higher quality and do not show any low-mass cut-off, facilitating a better identification of the actual phosphorylation sites when samples with low complexity are analyzed. However, the recent advantage of the data-dependent acquisition mode (41) for the orbitrap mass spectrometer in combination with its short duty cycle and superior sensitivity makes the latter instrument especially useful for the analysis of more complex samples, *i.e.* for a more comprehensive quantitative analysis of (phospho)peptides.

The overall purification strategy is depicted in Fig. 2*A*. As an example for obtained MS/MS spectra, Fig. 2*B* shows the spectrum of a tryptic peptide encompassing amino acids 186–223 of SLP-65 with a mass to charge ratio  $m/z = 1461,9528$  recorded on a Q-ToF mass spectrometer. The spectrum revealed that the peptide was singly phosphoryla-

ted at either position Tyr-194 or Tyr-205. Tyrosine phosphorylation was confirmed by the immonium ion at  $m/z = 216,04$  and the exact positions of both phosphorylation sites were verified by the corresponding fragment ions, which were either  $(b9 + 80)^{1+}$  for Tyr(P)-194 or  $(y27 + 80)^{3+}$  and  $(y27 + 80)^{2+}$  for Tyr(P)-205. Serine or threonine phosphorylation was not detected for this particular peptide. No loss of phosphoryl groups (98 atomic mass units) was observed for any of the serine/threonine-containing fragment ions in their different charge stages ( $y16^{(1+,2+)}$ ,  $y17^{(1+,2+)}$ ,  $y18^{(1+,2+)}$ ) and (b6 and b8). Of note, this particular phosphopeptide demonstrated a certain difficulty in MS-based phosphopeptide analysis. Although the peptide is singly phosphorylated, two phosphorylation sites are unambiguously identified, which has to be interpreted in a way that both phosphorylation states of this particular peptide are present at the same time. Importantly, such peptide mixtures can not be quantified (see below) as those peptides that are singly phosphorylated but on different residues have exactly the same mass and elute at the same time from the reverse phase column.

Fig. 3 shows the amino acid sequence of avian SLP-65 with all identified phosphorylation sites marked in *red*. We detected a total of 41 phospho-acceptor sites within SLP-65. The exact amino acid positions were mapped for 36 residues. We found 26 phosphoserine, 6 phosphothreonine, and 9 phosphotyrosine residues (see supplemental Table I for the entire list of phosphopeptides and supplemental Data 1 for annotated MS/MS spectra). For serine phosphorylation sites located within the amino acids 397 and 398 and between the amino acids 422 and 429, we could not determine their exact positions because of their close proximity but MS and MS/MS revealed that one of the two and four of the six serines were phosphorylated, respectively. With the single exception of Tyr-103 we confirmed all of the tyrosine phosphorylation sites previously reported and identified by manual Edman sequencing of <sup>32</sup>P-labeled SLP-65 or the use of phosphosite-specific antibodies (21). One reason why we may have missed Tyr(P)-103 in our analysis is the lack of arginine or lysine residues between amino acids 70 and 124. Therefore tryptic fragments, which covered that region of the protein and are of suitable length for MS and MS/MS analysis, could not be produced. However, phosphorylation of Tyr-103 was also not detected following digestion of SLP-65 with chymotrypsin. This might reflect species-specific differences between human and avian SLP-65. Alternatively and more probably, Tyr-103 phosphorylation is highly transient. Collectively, the detection of at least 41 phosphorylation sites reveals SLP-65 to be one of the most potent substrates for protein kinases known so far. The enormous degree of phosphorylation helps to explain how SLP-65 can function as the central relay to receive, process, and pass on BCR-derived signals.

**SLP-65 Phosphorylation Is Differentially Regulated over Time**—To learn more about the dynamics of SLP-65 phosphorylation as a basis for signal plasticity we wished to quan-

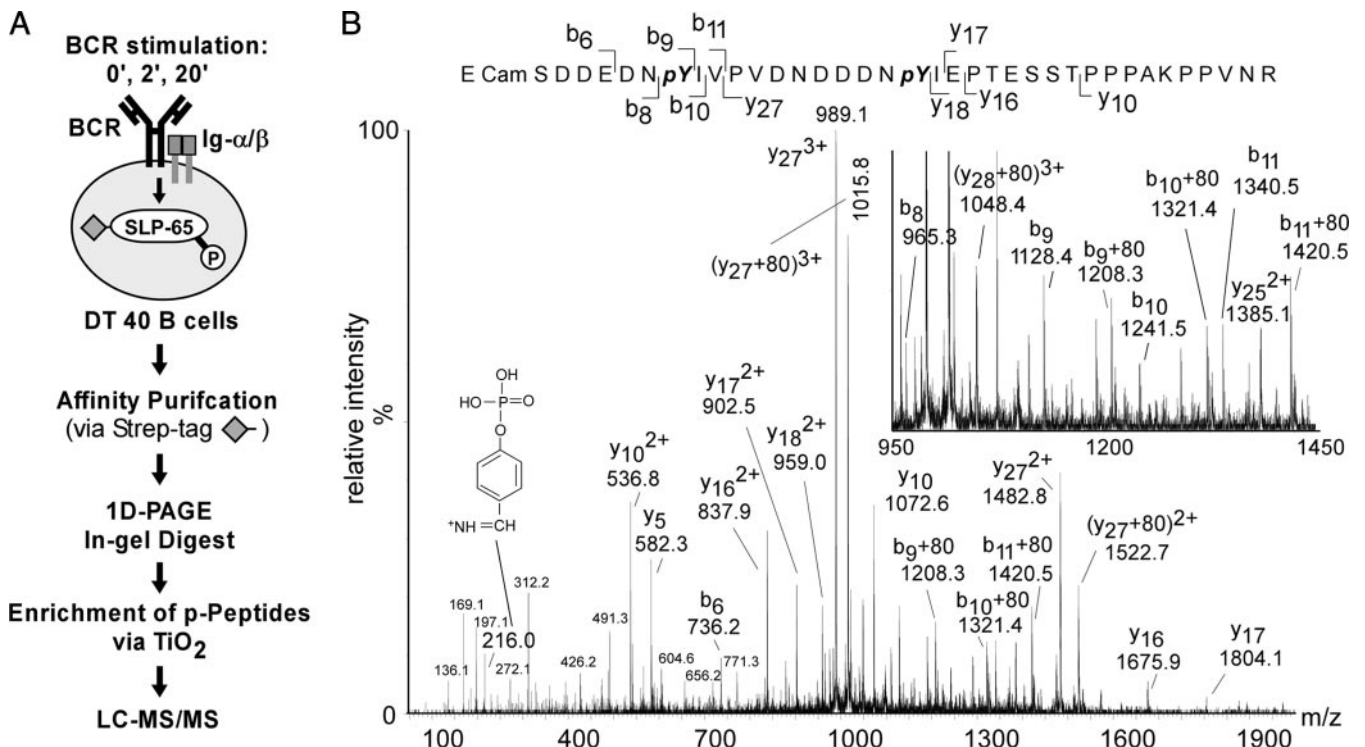


FIG. 2. Identification of SLP-65 phospho-acceptor sites. A, strategy for proteomic analysis of *in vivo* phosphorylation sites in SLP-65. Following BCR stimulation of DT40 B cells, peptide-tagged SLP-65 was affinity-purified, subjected to 1D-PAGE, and digested in the isolated gel slice with trypsin or chymotrypsin. Phosphopeptide products were enriched by TiO<sub>2</sub> chromatography and analyzed by liquid chromatography coupled to tandem mass spectrometry (LC-MS/MS). B, MS/MS spectrum of a quadruply charged and singly phosphorylated peptide (*m/z* 1461.9528) of SLP-65 in which tyrosines 194 (Y194) and 205 (Y205) are found to be phosphorylated (<sub>188</sub>SDDDEDNpYIVPVDNDDDNpYIEPTESSTPPPAKPPVNR<sub>223</sub>). Y-type and b-type fragment ions that identify unambiguously the two phosphorylation sites and the phosphotyrosine immonium ion (*m/z* = 216) are indicated.

```

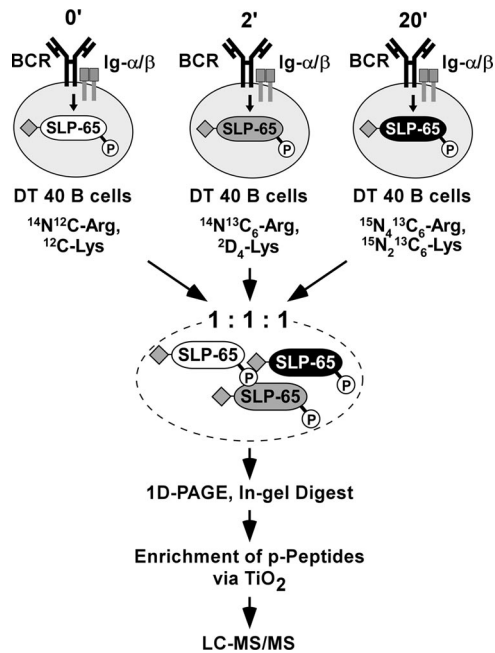
1 mdklnklavp agekfrklqk mvhdikknes giinkfkkkfq neqvalickt
51 gkdtdwdrkk kpppslprrd yasehadnee eqwSddfdsd Yenpdghsds
101 emYvvpseen pddSYeppps eqekkkips fpisrgeYad nrtshhqlpp
151 inkplpstps salprpkpS lpspaakpkl plkprecSdd ednYivpvdn
201 dddnYiepte sstpppakpp vnrfmkppak salptppkps lasdmqevye
251 vpeeeelSp ppvtrftkpl patraqnaeh shmsmtres pkldasrnl
301 plprnrllhp kdheannnde nhsfsntqes kfppggaapSp lpralkktsn
351 avnpakpclp srdtftvned kptaadrrrry SShefplppl psgtpksslq
401 kplvlpkvp apsraltgSp hssississt adqdagvhs k awYaatecdrk
451 TaedalYrsn kdgsflirks Sgqdsrqpvt lvvfynrrvy nipirfiest
501 rqyalgrekc geerfdsvae ivenhqhtsl vlidsqntk dstklkYivr
551 vS
    
```

FIG. 3. Phosphorylation sites in SLP-65. Amino acid sequence of SLP-65 from *Gallus gallus* with phosphorylation sites labeled as follows: Sites, which are conserved in *homo sapiens* are labeled with bold red capitals. Bold lowercase letters indicate species-specific sites. Red lowercase letters denote putative acceptor sites in phosphopeptides where the number but not the exact position could be identified unambiguously by MS. Tyrosine 103 that was previously identified as a phospho-acceptor site but was not seen in this study is labeled with a black bold capital letter.

tify the phosphorylation kinetics of individual sites by a 3-plex SILAC approach followed by MS-based analysis of tryptic SLP-65 phosphopeptides (42). The strategy is summarized in Fig. 4.

For metabolic protein labeling, DT40 cells expressing tagged SLP-65 were cultured in the presence of either light isotopes (<sup>12</sup>C<sub>6</sub>, <sup>14</sup>N<sub>2</sub>-Lys; <sup>12</sup>C<sub>6</sub>, <sup>14</sup>N<sub>4</sub>-Arg), intermediate isotopes (<sup>2</sup>D<sub>4</sub>, <sup>12</sup>C<sub>6</sub>, <sup>14</sup>N<sub>2</sub>-Lys, <sup>13</sup>C<sub>6</sub>, <sup>14</sup>N<sub>4</sub>-Arg), or heavy isotopes (<sup>13</sup>C<sub>6</sub>, <sup>15</sup>N<sub>2</sub>-Lys; <sup>13</sup>C<sub>6</sub>, <sup>15</sup>N<sub>4</sub>-Arg). Cells cultured with light iso-

topes were left untreated whereas those labeled with intermediate or heavy isotopes were BCR-stimulated for 2 and 20 min, respectively. Cleared cellular lysates were collected and pooled at a 1:1:1 ratio. Following 1D-PAGE, the SLP-65 protein band representing a stoichiometric mixture of SLP-65 molecules from the differently treated cells was excised and digested with trypsin. Resulting phosphopeptides were enriched by TiO<sub>2</sub> chromatography, analyzed by LC-MS/MS, and quantified by MSQuant as described in



**FIG. 4. Schematic representation of a 3-plex SILAC approach for profiling phosphorylation dynamics of SLP-65 in resting and activated B cells.** DT40 B cell transductants expressing SLP-65 with a N-terminal One-STrEP-Tag (◆) were cultured in medium with light, intermediate, or heavy amino acids as indicated and left untreated or BCR-activated for 2 or 20 min. Lysates were mixed in a 1:1:1 ratio. SLP-65 was affinity-purified, subjected to 1D-PAGE, and digested with trypsin in the isolated gel slice. Resulting phosphopeptide products were enriched by  $\text{TiO}_2$  chromatography and analyzed by LC-MS/MS. See “Results” for details.

Ref. 43. This approach allowed an unbiased relative quantification of SLP-65 phosphorylation in resting and stimulated cells because SLP-65 phosphopeptides derived from differently treated cells could be distinguished and hence unambiguously assigned to one of the three stimulation conditions by their distinct relative molecular masses. SLP-65 phosphopeptides obtained from resting B cells contained only light arginine and lysine residues. The arginine and lysine isotopes used for labeling cells that were subjected to BCR stimulation for 2 or 20 min were either 6 and 4 atomic mass units or 10 and 8 atomic mass units heavier, respectively. The complete SLP-65 phosphopeptide quantification obtained from six independent experiments is shown in Table I. Annotated MS and MS/MS spectra and a table displaying all quantifications are shown in the supplemental data (supplemental Table II and supplemental Data 2 for annotated spectra). Of note, it has been reported that deuterium-labeled peptide species elute earlier from the column under reversed phase conditions as the corresponding non-labeled peptides (44). Such differentially eluting species should not be quantified by MS. However, we did not observe this particular effect for labeled peptides in our experiments. As exemplified for a singly phosphorylated peptide that carries three lysine residues (*i.e.* 12 deuterium

atoms), no difference in the elution time from the reversed column could be detected (see supplemental Data 3).

The quantitative data revealed that the SLP-65 phosphorylation sites previously identified in our qualitative analysis were engaged in a differential and highly complex manner. We grouped the phospho-acceptor sites into different categories according to their BCR-induced phosphorylation/dephosphorylation kinetics; immediate early and transient sites, early and sustained sites, late sites, and down-regulated sites, which were already phosphorylated in the resting B cell but underwent rapid and sustained dephosphorylation in response to BCR activation. We also mapped constitutively phosphorylated sites that were unaffected by the BCR. Fig. 5 lists distinct SLP-65 phosphorylation sites assigned to each of these categories.

Consistently with the role of SLP-65 tyrosine phosphorylation for signal initiation (25), most of the tyrosine phosphorylation sites identified (Fig. 3, see above) were found to belong to the first category, *i.e.* their phosphorylation took place soon upon BCR stimulation and declined thereafter (Fig. 5A). None of the phosphotyrosine sites was found to be engaged in the absence of BCR activation or to be a late responder. Remarkably, Tyr-457 remained phosphorylated even at 20 min upon BCR activation (Fig. 5B).

The most frequently detected phosphopeptide was  $^{168}\text{KPSLPSPAAPK}^{179}$ . Of the two phospho-acceptor sites, Ser-170 and Ser-173, only the first one is evolutionarily conserved including human SLP-65 (see supplemental Data 5). As shown in Table I, singly as well as doubly phosphorylated forms were observed. Fig. 6A shows that the amount of the singly phosphorylated peptide decreased slightly upon BCR stimulation (Table I and Fig. 6A), whereas the amount of the doubly phosphorylated peptide increased over time (C). Close inspection of the MS/MS spectra revealed that singly phosphorylated peptides contained exclusively Ser(P)-173 but not Ser(P)-170 (Fig. 6B). The Ser-173-containing fragment ions  $\gamma 7$ -( $p$ SPKAAKPK $^+$ ),  $\gamma 8$ -( $p$ SPKAAKPK $^+$ ), and  $\gamma 9$ -( $p$ SPKAAKPK $^+$ ) showed unambiguously a neutral loss of ( $\gamma 7 - 98$ ) $^+$ , ( $\gamma 8 - 98$ ), ( $\gamma 9 - 98$ ) $^+$ . The  $b_4$  ion (KPSL $^+$ ) harboring Ser-170 was observed only in its non-phosphorylated form, *i.e.* no ( $b_4 - 98$ ) ion could be assigned (Fig. 6C). Importantly, in the extracted ion chromatogram of the  $m/z$  value of the singly phosphorylated peptide and its isotopically labeled counterparts, only one sharp peak could be observed at a defined retention time (supplemental Data 3). MS/MS of the co-eluting labeled counterparts again revealed that only Ser-173, and not Ser-170, was phosphorylated within this peptide species (supplemental Data 4). The MS/MS spectra of the doubly phosphorylated peptide again revealed phosphorylation of Ser-173 (( $\gamma 8 - 98$ ) $^+$ ) but also exhibited  $b$ -type fragment ions  $KPpSL^+$  and  $KPpS^+$  with a loss of phosphoric acid derived from Ser(P)-170, *i.e.* ( $b_4 - 98$ ) $^+$  and ( $b_3 - 98$ ) $^+$ , respectively (Fig. 6D). In summary, the basic observation of a stimulation-dependent enrichment of the doubly phosphorylated peptide does *per se*

TABLE I  
Relative quantification of phosphopeptides

MS-based relative quantification of tryptic SLP-65 phosphopeptides obtained from DT40 B cells, which were left untreated or BCR-stimulated for 2 or 20 minutes. The table lists the sequence, molecular weight (MW) and charge state (*n*) of the phosphopeptides, the MASCOT peptide score, the number of sites (no.), their exact positions (site), the number of biological replicates (R), the quantitative ratio of 0 versus 2 min (0'/2') and 0 versus 20 min (0'/20') as determined by MSQuant, and the standard deviation(s) (STD). Those values, which were calculated from peptides that could be quantified with only one biological sample, are marked with an *asterisk*. In those cases STD refers to values that were obtained solely by the number of MS scans used for relative quantification in the MSQuant program. A *double-asterisk* represents the mean value of the STD of two experiments. Phosphosites that were unambiguously identified by manual inspection of the MS/MS spectra are shown in bold black italic capitals (**pS/pT/pY**). Peptides with one or two phosphorylation sites that could not be identified unambiguously are shown in bold black italic lower-case letters (**s/t/y**). Table with all sequences and values used for calculation and the manually annotated MS/MS spectra of the quantified peptides are shown in the supplemental data.

Peptide	MW (+n)	Score	Site	No.	R	0'/2'	STD 0'/2'	0'/20'	STD 0'/20'
TGKD <b>p</b> TWDR	1057,4681 (+2)	24	Thr-54	1	1	2.6*	0.1*	1.6*	0.4*
KKPPP <b>p</b> SLPR	1098,6314 (+3)	38	Ser-65	1	3	2.2	0.6	1.3	0.2
IP <b>S</b> pSFPISR	1082,5360 (+2)	35	Ser-130	1	3	4.9	0.9	4.7	0.7
KIPSSFPISRGE <b>p</b> YADNR	2016,0122 (+3)	14	Tyr-138	1	1	12.9*	1.6*	5.5*	1.0*
KPSLP <b>p</b> SPAAPKPK	1299,6942 (+3)	53	Ser-173	1	5	0.7	0.1	0.8	0.06
KP <b>p</b> SLP <b>p</b> SPAAPKPK	1379,6617 (+2)	42	Ser-170, Ser-173	2	6	1.8	0.3	2.3	0.2
ECamSDEEDNIYVPVDNDDDN <b>p</b> YIEPTESSTPPPAKPPVNR	4382,8776 (+3)	45	Tyr-205	1	1	9.2*	3.5*	4.5*	1.9*
ECampSDEEDN <b>p</b> YIVPVDNDDDN <b>p</b> YIEPTESSTPPPAKPPVNR	4542,8170 (+3)	48	Ser-188, Tyr-194, Tyr-205	3	1	10.1*	–	2.3*	–
ECampSDEEDNIYVPVDNDDDN <b>YIEP</b> tEsstPPPAKPPVNR	4462,7997 (+3)	27	Ser-188, Thr-209/ Ser-211/Ser-212/ Thr-213	2	1	0.9*	0.1*	1.3*	0.2*
ECcamSDEEDNIYVPVDNDDDN <b>YIEPT</b> ESS <b>p</b> TTPPAKPPVNR	4382,8390 (+3)	52	Thr-213	1	1	1.7*	0.2*	2.3*	0.2*
SALPTPPKPSLASDMQEV <b>p</b> YEVPEEEEEELSPPPVTR	3927,8283 (+3)	42	Tyr-249	1	1	0.9*	0.2*	1.8*	0.4*
SALPTPPKPSLASDMoxQEVYEVPEEEEEEL <b>p</b> SPPPVTR	3943,8529 (+3)	64	Ser-259	1	5	1.2	0.1	2.1	0.3
SALP <b>p</b> TTPKPSLASDMoxQEVYEVPEEEEEEL <b>p</b> SPPPVTR	4023,7866 (+3)	25	Thr-235, Ser-259	2	1	1.0*	0.1*	0.9*	0.1*
AQNAEHSHMoxHpSMTRES <b>p</b> K	2188,8773 (+4)	21	Ser-285	1	2	0.4**	0.04**	0.3**	0.05**
E <b>p</b> SPKLDASR	1081,4620 (+2)	49	Ser-290	1	5	0.5	0.1	0.5	0.1
FPPGAAP <b>p</b> SPLPR	1285,6433 (+2)	54	Ser-339	1	4	1.0	0.2	0.6	0.2
RG <b>p</b> SSHEFFLPLPSGTPK	1983,0084 (+3)	42	Ser-381	1	3	3.2	0.5	3.1	0.5
RG <b>p</b> SSHEFFLPLPSG <b>p</b> TPK	2062,9731 (+3)	32	Ser-381, Thr-394	2	2	3.3	0.7**	1.8	0.4**
sslQKPLVLPK	1288,7360 (+2)	23	Ser-397/Ser-398	1	3	4.7	0.6	7.1	4
ALGT <b>p</b> SPHSSISSISSTADQDAGVHSK	2621,1562 (+2)	85	Ser-419	1	2	1.1	0.1	1.5	0.2
ALGT <b>s</b> PHSSISSISSTADQDAGVHSK	2701,1458 (+3)	62	Ser-419/Ser-422/ Ser-423	2	4	1*	0.2*	1.6*	0.3*
TAEDAL <b>p</b> YR	1021,4243 (+2)	44	Tyr-457	1	1	5.0*	0.7*	6.3*	1.7*
K <b>S</b> pSGQDSR	943,3749 (+2)	22	Ser-471	1	1	1.2*	0.2*	6.1*	0.83*

not allow one to determine which of the two serine residues undergoes inducible phosphorylation. In conjunction with the absence of the Ser-170 mono-phosphate version in our preparations (see above) the available data suggest strongly that BCR-triggered kinases act mainly on Ser-170, which appears to be a particularly sensitive substrate. Classification of phosphorylation at Ser-173 at this stage of our analysis was more difficult. Most probably it is already phosphorylated in resting cells but stimulation-dependent phosphorylation of Ser-170 might convert the singly phosphorylated peptide into its doubly phosphorylated form (see Fig. 4). This could explain why the amount of the peptide containing only Ser(P)-173 is reduced upon receptor stimulation whereas the amount of the doubly phosphorylated form is increased at the same time (Fig. 4D). Interestingly, a highly dynamic phosphorylation turnover can occur at two acceptor sites that are separated by only two amino acids.

*The DT40 Cell System Allows in Vivo Evaluation of Phosphoproteomic Results*—Next we wanted to complement our

quantitative phosphorylation analysis by functional studies within the same cellular system. Indeed, the DT40 reconstitution approach provides such an advantageous possibility. To elucidate the signal significance of the newly identified Ser-170 and Ser-173 phosphorylation sites, we generated retroviral expression constructs encoding SLP-65 variants in which the particular serine residues were exchanged for alanine and which, moreover, contained at their N terminus the green fluorescent protein (GFP). As control, we used GFP-tagged wild-type SLP-65. The GFP tag allowed us to ensure equal levels of protein expression upon transduction of the vectors into SLP-65-negative DT40 mutants by flow cytometry (Fig. 7A, left panel). The retroviral transfer method was chosen to prevent individual variations of the signaling capability of single cell clones. Equal BCR expression of the transduced DT40 cells was checked separately by flow cytometry (Fig. 7A, right panel).

To confirm biochemically the phosphorylation of Ser-170, DT40 transductants were subjected to BCR activation for

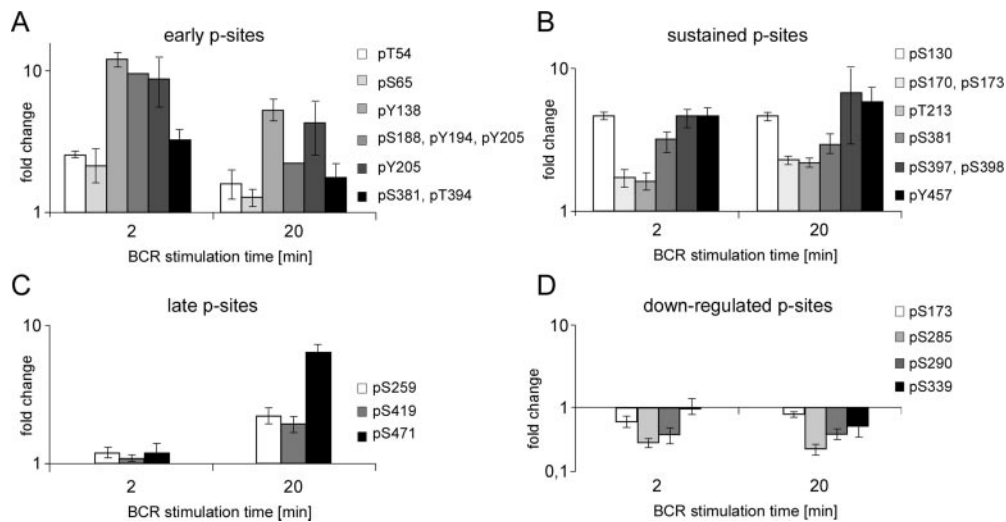


**FIG. 5. Classes of differentially phosphorylated acceptor sites in SLP-65.** *A*, phosphorylation at early and transient acceptor sites occur within the first 2 min upon BCR activation and declines thereafter. *B*, early and sustained acceptor sites remain phosphorylated even 20 min following BCR activation. *C*, late acceptor sites undergo phosphorylation upon 20 min of BCR activation. *D*, down-regulated acceptor sites are phosphorylated already in resting cells and undergo BCR-induced dephosphorylation. Note that phosphorylation of constitutive acceptor sites is unchanged in resting and BCR-activated B cells and is therefore not shown in this figure. Error bars indicate the standard deviations of the obtained fold changes for each phosphorylated residue at each time-point.

different time periods. Subsequently, wild-type SLP-65 and the S170A mutant form were immunopurified from the lysates by anti-GFP antibodies. Purified proteins were analyzed by immunoblotting with a phosphosite-specific antibody recognizing the consensus sequence R/KXXpSXP (Fig. 7*B*, upper panel). Consistently with our quantitative MS data, Ser-170 phosphorylation occurred after 2 min of BCR stimulation and persisted for at least 20 min. Ser-170 phosphorylation was absent in the S170A mutant variant (Fig. 7*B*, upper panel, lanes 1–5 and 11–15, respectively). The efficiency of the immunoprecipitation and equal protein loading was confirmed by reprobing the membrane with anti-SLP-65 antibodies (Fig. 7*B*, lower panel).

Our MS data showed that in contrast to BCR-induced phosphorylation of Ser-170, phosphorylation of Ser-173 is already present in resting B cells. However, Ser-170 phosphorylation was only found in combination with phosphorylation of Ser-173. These findings prompted us to investigate whether Ser-170 phosphorylation depends on preceding phosphorylation of Ser-173. Therefore we included the S173A mutant form of SLP-65 in our phosphorylation analysis (Fig. 7*B*, upper panel, lanes 6–10). BCR-induced phosphorylation of Ser-170 was severely compromised for the S173A mutant (Fig. 7*B*, upper panel) demonstrating that Ser-170 serves as a kinase substrate only in the presence of Ser(P)-173. Neither global tyrosine phosphorylation of SLP-65 nor its particular phosphorylation at the PLC- $\gamma$ 2 binding sites, *i.e.* Tyr-194 and Tyr-205 (21), was affected by the S173A exchange (Fig. 7*B*, middle panel and data not shown).

*Ser-170 Phosphorylation Is a Specific Signal Modifier for the Activation of p38/JNK and AP1*—The effect of the con-

certed Ser-170/Ser-173 phosphorylation on BCR-induced signaling was assessed at the level of early as well as late events. As revealed by anti-phosphotyrosine immunoblotting (Fig. 8*A*), lack of Ser-170 phosphorylation in cells expressing the corresponding mutant form of SLP-65 impaired neither the quality nor the kinetics of global protein tyrosine phosphorylation (lanes 9–12) compared with that observed in cells expressing wild-type SLP-65 (lanes 1–4). Lack of phosphorylation of Ser-173 altered global tyrosine phosphorylation marginally (lanes 5–8). This was further confirmed by immunoblotting against specific kinase substrates such as Syk, Lyn, or Dok-3 (data not shown). Furthermore, the BCR-induced  $\text{Ca}^{2+}$  response was equally well supported by wild-type SLP-65 and both of its mutant forms (Fig. 8*B*). In contrast, striking and selective differences were observed for the inducible activation of the three MAP kinases Erk, p38, and JNK, which was monitored by immunoblot analysis with antibodies directed against their phosphorylated forms. Although stimulation of Erk activity turned out to be independent of Ser-170 phosphorylation (Fig. 9*A*), the phosphorylation and hence activation of p38 and JNK were drastically diminished in cells expressing the S170A mutant (Fig. 9, *B* and *C*, respectively). Similar results were obtained for cells expressing the S173A mutant (data not shown). Hence Ser-170/Ser-173 phosphorylation of SLP-65 modulates some but not all cytosolic signaling events in response to BCR activation.

MAP kinases are upstream regulators of the transcription factor AP1, which plays a major role in the development and function of B cells (28). This prompted us to investigate AP1 activation in our SLP-65 transductants and thereby to test



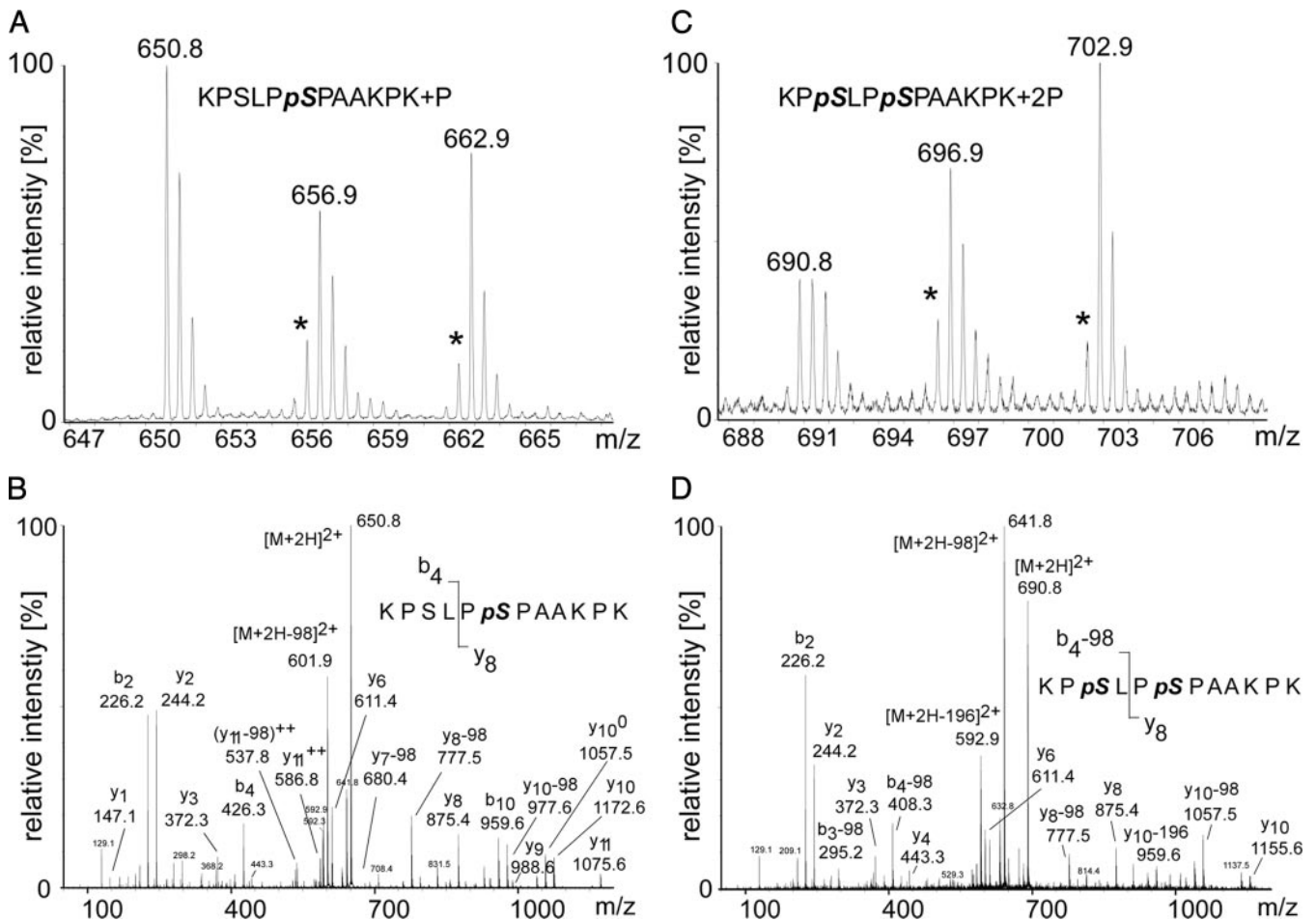


**FIG. 6. MS-based relative quantification of the most frequently detected SLP-65 phosphopeptide encompassing amino acids 168–179.** A, MS spectrum of the singly phosphorylated peptide  ${}_{168}\text{KPSLPpSPAACKPK}_{179}$  ( $m/z = 650.8$ ) containing Ser(P)-173 in unstimulated cells. Note the reduced peak intensity values for the peptides ( $m/z = 656.9$ ,  $m/z = 662.9$ ) obtained from cells stimulated through their BCR for 2 or 20 min, respectively. This indicates either BCR-induced dephosphorylation or conversion of the singly phosphorylated form into the doubly phosphorylated form. Intensities of mass peaks labeled with an asterisk might be slightly reduced due to a certain impurity of the isotope-labeled amino acids. B, Y-type and b-type fragment ions in the MS/MS spectrum show unambiguously that singly phosphorylated versions of the peptide 168–179 contain only Ser(P)-173 but not Ser(P)-170. C, MS spectrum of the doubly phosphorylated peptide ( ${}_{168}\text{KPpSLPpSPAACKPK}_{179}$ ;  $m/z = 690.8$ ) harboring both Ser(P)-170 and Ser(P)-173. Comparison of the peak intensities of unlabeled and labeled peptides reveals a stimulation-dependent enrichment of the doubly phosphorylated peptide indicating BCR-induced phosphorylation. D, Y-type and b-type fragment ions in the MS/MS spectrum of the doubly phosphorylated peptide  ${}_{168}\text{KPpSLPpSPAACKPK}_{179}$  unambiguously reveal that both serines 170 and 173 are phosphorylated.

whether Ser-170/Ser-173-mediated signal modulation in the cytosol also translates into altered nuclear responses. To monitor AP1-regulated gene transcription we equipped our transductants with an AP1-driven luciferase reporter gene construct. Empty vector-transfected cells served as control, and co-transfection of a  $\beta$ -galactosidase expression plasmid allowed the normalization of reporter gene activity according to the transfection efficiencies. As shown in Fig. 9D and as reported earlier (29), AP1-mediated induction of gene expression was strictly dependent on SLP-65. Compared with wild-type SLP-65, the S170A and the S173A mutants were strikingly less potent in promoting this response causing a dramatically reduced transcription of the reporter gene construct after 6 h of BCR activation (Fig. 9D,

open and black bars). The level of reduction in the mutant cells was almost identical to that achieved by pharmaceutical inhibition of JNK in cells expressing wild-type SLP-65 (Fig. 9, light gray bars). Moreover, administration of the JNK inhibitor to cells expressing the S170A or the S173A mutant did not further reduce reporter gene activity. Our AP1 reporter gene assay was less sensitive to inhibition of p38 (Fig. 9D, gray bars). Taken together these findings demonstrate a hierarchical phosphorylation of the Ser-170/Ser-173 kinase substrate sites in that sustained phosphorylation of Ser-170 depends on preceding phosphorylation of Ser-173. Once phosphorylated Ser-170 provides a selective amplification of cytosolic and nuclear signaling events upon BCR activation.

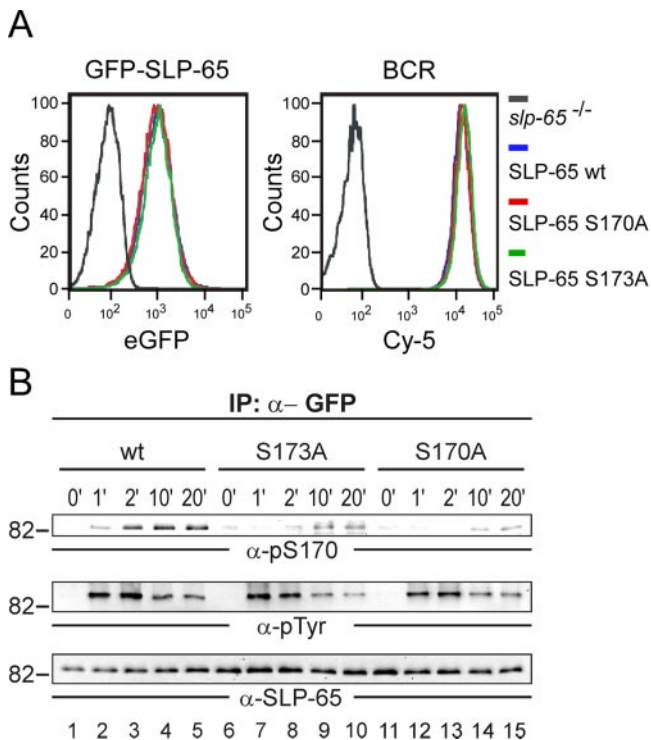


**FIG. 7. Expression of wild-type SLP-65 as well as its S170A- and S173A mutant forms with an N-terminal GFP moiety.** A, SLP-65-deficient DT40 B cells were subjected to retroviral transduction inducing stable expression of a GFP fusion protein encompassing either wild-type SLP-65 (GFP-SLP-65) or mutant SLP-65 variants in which either serine 170 or serine 173 was replaced by alanine (GFP-SLP-65-S170A or -S173A). GFP-positive cells were isolated by fluorescence-activated cell sorting to achieve populations expressing equal amounts of GFP-SLP-65 (left panel). Equal BCR expression of the obtained cell populations was confirmed by flow cytometry using Cy-5-labeled anti-IgM antibodies (right panel). B, cells described in A were left untreated (0 min; lanes 1, 6, and 11) or BCR-stimulated for indicated times in minutes (lanes 2–5, 7–10, 12–15). From cleared cellular lysates GFP-SLP-65 proteins were purified by anti-GFP immunoprecipitation, and obtained proteins were analyzed by immunoblotting with anti-Ser(P)-170, anti-Tyr(P), and anti-chicken SLP-65 antibodies (upper, middle, and lower panel, respectively).

#### DISCUSSION

With this study we have introduced the DT40 reconstitution system as a useful tool to combine qualitative and quantitative phosphoproteomic analyses with functional genomics. This approach allowed purification of the target protein, acquisition of proteomic data sets, and subsequent elucidation of their biological significance in a single cellular system. In fact, DT40 cells have already been employed in a large number of signaling studies (45). The use of DT40 cells as a model system was fostered principally by two considerations. Firstly, exogenously introduced gene fragments integrate homologously into the DT40 host genome with high frequency (35). This property supports gene targeting experiments and the generation of loss-of-function mutants. Secondly, restoration of the original signaling phenotype by transfection experiments re-

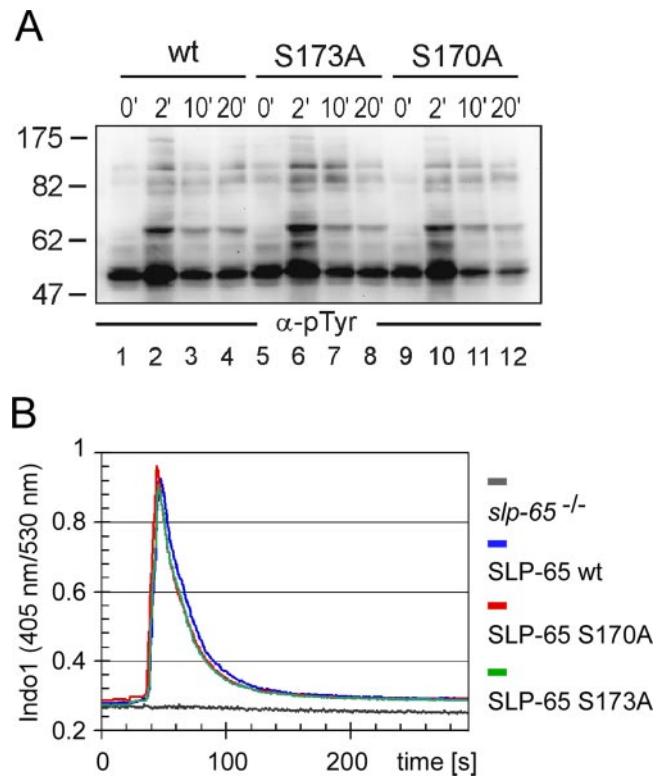


**FIG. 8. Phosphorylation of serine 170 or serine 173 does not affect early BCR signaling events.** A, DT40 B cells expressing either wild-type, S173A, or S170A mutant GFP-SLP-65 (as described in the legend to Fig. 7A) were left untreated (0 min; lanes 1, 5, and 9) or stimulated for 2 min (lanes 2, 6, and 10), 10 min (lanes 3, 7, and 11), or 20 min (lanes 4, 8, and 12) through their BCR. Induction of global protein tyrosine phosphorylation was monitored by anti-phosphotyrosine immunoblotting of cleared cellular lysates. B, cells described in A were loaded with the ratiometric  $\text{Ca}^{2+}$  chelating dye Indo-1 and subsequently stimulated through their BCR. Induction of intracellular  $\text{Ca}^{2+}$  mobilization was recorded by flow cytometry calculating the ratio between Indo-1 blue (405 nm) and Indo-1 violet (530 nm) for normalizing the results according to the loading efficiency. Curves represent intracellular  $\text{Ca}^{2+}$  concentrations of stimulated cells expressing no SLP-65 (gray), wild-type GFP-SLP-65 (blue), GFP-SLP-65-S170A (red), and GFP-SLP-65-S173A (green).

vealed that the molecular mechanisms by which effector proteins execute their function are highly conserved during evolution. For example, the early block of BCR signaling in Syk- or SLP-65-deficient DT40 cells is fully restored by reconstituting these cells with the corresponding homologues of other species (46). Also other disease-related processes, notably mechanisms of cell death, have been successfully addressed in the DT40 model system (47, 48). Collectively these features promote using the DT40 system for functional proteomic studies on different aspects of general cell biology.

Our target protein in this study was the cytoplasmatic BCR effector SLP-65, which is a prototype of receptor-proximal transducer elements. We showed that SLP-65 possesses at least 41 phospho-acceptor sites. Such a high number of phosphorylation sites are rarely found in other phosphopro-

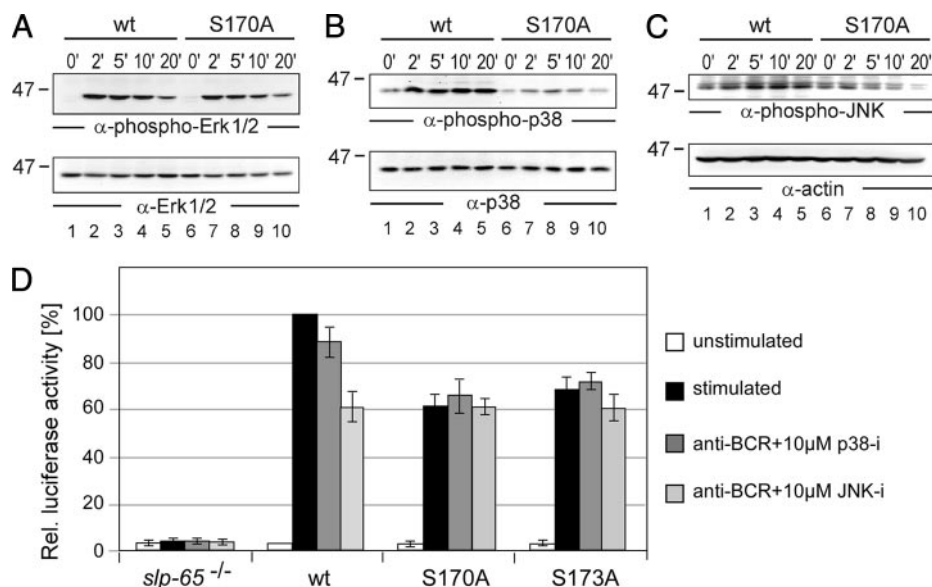


**FIG. 9. Phosphorylated serines 170 and 173 serve as a distal switch for the activation of MAP kinases p38/JNK and the AP1 transcription factor.** DT40 B cells expressing GFP-tagged versions of wild-type SLP-65 (lanes 1–5) or S170A mutant SLP-65 (lanes 6–10) were investigated for their ability to activate distinct MAP kinase family members upon BCR engagement for the indicated times by immunoblot analysis of cleared cellular lysates with antibodies against (A) phospho-Erk, (B) phospho-p38, and (C) phospho-JNK (upper panels). Protein loading was monitored by immunoblotting with antibodies against Erk, p38, and actin, respectively (lower panels). D, SLP-65-deficient DT40 cells and those cells expressing wild-type SLP-65 or its mutant forms S170A or S173A were monitored for their ability to activate transcription of an AP1-driven luciferase reporter gene by co-transfection of an AP1 reporter construct with a  $\beta$ -galactosidase expression plasmid followed by determination of enzyme activities in untreated cells (white bars) and cells stimulated through their BCR for 6 h (black bars). Where indicated (dark gray and light gray bars), cells were pretreated with inhibitors of either p38 or JNK one hour before stimulation. Three independent experiments were performed, and data were normalized according to transfection efficiencies.

teins. Among the SLP-65 phosphosites, a majority of 63% was assigned to serine residues. Tyrosine residues constitute 22% of the total reservoir whereas 15% involve threonine residues. As revealed by global phosphoproteome analysis (34), the average distribution of phosphoamino acids in eukaryotic cells is 86% for phosphoserine and 12% for phosphothreonine. Only about 2% of the phosphorylation events occur on tyrosine. The relatively high proportion of phosphotyrosine residues in SLP-65 reflects the proximal position of this adaptor to the activated BCR and its associated protein tyrosine kinase Syk, which provides the enzymatic activity for the onset of signaling (49).

Quantification of the phosphorylation events revealed five categories of phosphosites based on their phosphorylation/dephosphorylation kinetics in the absence or presence of BCR activation. Phosphorylation at immediate early and transient sites occurs within the first 2 min of BCR activation and declines thereafter. In contrast, early and sustained sites remain phosphorylated even after 20 min of stimulation, when late sites become engaged. SLP-65 also possesses down-regulated phosphorylation sites, which show inducible dephosphorylation by protein phosphatases. Finally, phosphorylation of constitutive sites does not differ between resting and BCR-activated cells.

In all, we were able to quantify 23 distinct phosphopeptides carrying 24 different phosphorylation sites (Table I) out of the

36 sites for which the actual position was identified unambiguously in the initial, qualitative experiments. The complete quantification of all sites was hampered by the following issues: (i) In the initial experiments some phosphorylation sites were detected after the samples had been digested with chymotrypsin or a mixture of chymotrypsin and trypsin (see supplemental Table 1). These peptides do not carry a labeled lysine or arginine at their C terminus and are thus not useful for quantification. (ii) For some peptides that were singly or doubly phosphorylated, more distinct phosphorylation sites were identified (see also Fig. 2B), as these peptides represented a mixture of the respective singly or doubly phosphorylated peptides. Consequently, these phosphopeptides could not be quantified. (iii) More phosphorylation sites were necessarily identified in the qualitative analysis because of the fact that in quantitative experiments three differently labeled samples were pooled with a consequent and inevitable increase in the complexity of the mass spectra. Because only the ten most prominent precursors in each MS scan were selected for MS/MS, those phosphopeptides (together with their labeled counterparts) that showed a relatively weak intensity had not necessarily been selected for sequencing in the quantitative experiments.

In our functional analyses we focused on the most frequently detected phosphopeptide encompassing amino acids 168–179. Two adjacent phosphosites could be as-

signed, *i.e.* serines at positions 170 and 173. Qualitatively we identified a mono-phosphate as well as the bis-phosphate form. Only phosphorylated Ser-173 was already present in resting B cells. A singly phosphorylated peptide in which only Ser-170 was phosphorylated could not be detected under any stimulation condition. Complementing our proteomic analysis by mutational reconstitution studies eventually allowed us to show that Ser-173 phosphorylation is a prerequisite for phosphorylation at Ser-170. This hierarchical phosphorylation cascade functions as a  $\text{Ca}^{2+}$ -independent amplification for the selective activation of MAP kinases p38 and JNK and the transcription factor AP1. Hence, SLP-65 can regulate B cell signaling cascades at several levels, *i.e.* upstream and downstream of PLC- $\gamma$ 2 activation. Consequently our data show that signal initiation and its distinct processing can emanate from differential modification of a single transducer element by phosphorylation. Especially hierarchical phosphorylation cascades within a given protein have been described as facilitating signal integration processes of different pathways (50, 51) This might create a basis for signal plasticity, which is particularly important for the adjustment of antigen receptor signaling in lymphocytes. For example, the quality and kinetics of inducible Ser-170 phosphorylation might be controlled selectively by positive BCR co-receptors such as CD19 (52, 53) or by negative ones such as CD22 (54, 55). Also the basal phosphorylation status of Ser-173 in resting B cells might be a subject of regulation. Further proteomic studies in the DT40 system will be needed to decipher the Ser-170/Ser-173 signaling network and eventually to elucidate the complete set of SLP-65 interaction partners including those regulated by serine/threonine phosphorylation.

In summary, we have established that differential and dynamic engagement of numerous phospho-acceptor sites enables SLP-65 to act as a master regulator that is responsible not only for early signal onset but also for later signal processing. This allows us to propose a functional definition of a signal integrator, *i.e.* a single effector protein acquires the ability to regulate several levels of signal transmission depending on its dynamic post-translational modifications.

**Acknowledgments**—We thank Victor Armstrong for critical review of the manuscript; Johanna Lehne, Uwe Plessmann, and Monika Raabe for excellent technical help in MS analysis; Carla Schmidt for help in the statistical validation of quantitative proteomic data; and Hanibal Bohnenberger for fruitful discussions.

\* This work was supported, in part, by the program of new emerging science and technology (NEST) of the European Union through Grant HYBLIB.

☐ The on-line version of this article (available at <http://www.mcponline.org>) contains supplemental material.

§ Funded by the Max Planck Institute for Biophysical Chemistry (MPI-BPC) and performed experiments at the Georg August University and the Max Planck Institute for Biophysical Chemistry.

\*\* Supported by the Alfred Benzoni Foundation.

‡ To whom correspondence may be addressed. Ph.: 49-551-

2011060; Fax: 49-551-2011197; E-mail: [henning.urlaub@mpi-bpc.mpg.de](mailto:henning.urlaub@mpi-bpc.mpg.de).

§§ To whom correspondence may be addressed. Ph.: 49-551-395821; Fax: 49-551-395843; E-mail: [jwienan@gwdg.de](mailto:jwienan@gwdg.de).

#### REFERENCES

- Pawson, T. (2007) Dynamic control of signaling by modular adaptor proteins. *Curr. Opin. Cell Biol.* **19**, 112–116
- Abram, C. L., and Lowell, C. A. (2007) The expanding role for ITAM-based signaling pathways in immune cells. *Sci. STKE* **2007**, 377
- Harwood, N. E., and Batista, F. D. (2008) New insights into the early molecular events underlying B cell activation. *Immunity* **28**, 609–619
- Le Clainche, C., and Carlier, M. F. (2008) Regulation of actin assembly associated with protrusion and adhesion in cell migration. *Physiol. Rev.* **88**, 489–513
- Delon, I., and Brown, N. H. (2007) Integrins and the actin cytoskeleton. *Curr. Opin. Cell Biol.* **19**, 43–50
- Glynn, R., Ghandour, G., Rayner, J., Mack, D. H., and Goodnow, C. C. (2000) B-lymphocyte quiescence, tolerance and activation as viewed by global gene expression profiling on microarrays. *Immunol. Rev.* **176**, 216–246
- Okkenhaug, K., and Vanhaesebroeck, B. (2003) PI3K in lymphocyte development, differentiation and activation. *Nat. Rev. Immunol.* **3**, 317–330
- Cullen, P. J., and Lockyer, P. J. (2002) Integration of calcium and Ras signaling. *Nat. Rev. Mol. Cell Biol.* **3**, 339–348
- Acuto, O., Di Bartolo, V., and Micheli, F. (2008) Tailoring T-cell receptor signals by proximal negative feedback mechanisms. *Nat. Rev. Immunol.* **8**, 699–712
- Rudd, C. E. (1999) Adaptors and molecular scaffolds in immune cell signaling. *Cell* **96**, 5–8
- Wu, J. N., and Koretzky, G. A. (2004) The SLP-76 family of adapter proteins. *Semin Immunol.* **16**, 379–393
- Wienands, J., Schweikert, J., Wollscheid, B., Jumaa, H., Nielsen, P. J., and Reth, M. (1998) SLP-65: a new signaling component in B lymphocytes which requires expression of the antigen receptor for phosphorylation. *J. Exp. Med.* **188**, 791–795
- Fu, C., Turck, C. W., Kurosaki, T., and Chan, A. C. (1998) BLNK: a central linker protein in B cell activation. *Immunity* **9**, 93–103
- Goitsuka, R., Fujimura, Y., Mamada, H., Umeda, A., Morimura, T., Uetsuka, K., Doi, K., Tsuji, S., and Kitamura, D. (1998) BASH, a novel signaling molecule preferentially expressed in B cells of the bursa of Fabricius. *J. Immunol.* **161**, 5804–5808
- Koretzky, G. A., Abtahian, F., and Silverman, M. A. (2006) SLP76 and SLP65: complex regulation of signaling in lymphocytes and beyond. *Nat. Rev. Immunol.* **6**, 67–78
- Jumaa, H., Wollscheid, B., Mitterer, M., Wienands, J., Reth, M., and Nielsen, P. J. (1999) Abnormal development and function of B lymphocytes in mice deficient for the signaling adaptor protein SLP-65. *Immunity* **11**, 547–554
- Pappu, R., Cheng, A. M., Li, B., Gong, Q., Chiu, C., Griffin, N., White, M., Sleckman, B. P., and Chan, A. C. (1999) Requirement for B cell linker protein (BLNK) in B cell development. *Science* **286**, 1949–1954
- Hayashi, K., Nittono, R., Okamoto, N., Tsuji, S., Hara, Y., Goitsuka, R., and Kitamura, D. (2000) The B cell-restricted adaptor BASH is required for normal development and antigen receptor-mediated activation of B cells. *Proc. Natl. Acad. Sci. U.S.A.* **97**, 2755–2760
- Xu, S., Tan, J. E., Wong, E. P., Manickam, A., Ponniah, S., and Lam, K. P. (2000) B cell development and activation defects resulting in *xid*-like immunodeficiency in BLNK/SLP-65-deficient mice. *Int. Immunol.* **12**, 397–404
- Engelke, M., Engels, N., Dittmann, K., Stork, B., and Wienands, J. (2007) Ca(2+) signaling in antigen receptor-activated B lymphocytes. *Immunol. Rev.* **218**, 235–246
- Chiu, C. W., Dalton, M., Ishiai, M., Kurosaki, T., and Chan, A. C. (2002) BLNK: molecular scaffolding through 'cis'-mediated organization of signaling proteins. *EMBO J.* **21**, 6461–6472
- Kohler, F., Storch, B., Kulathu, Y., Herzog, S., Kuppig, S., Reth, M., and Jumaa, H. (2005) A leucine zipper in the N terminus confers membrane association to SLP-65. *Nat. Immunol.* **6**, 204–210
- Abudula, A., Grabbe, A., Brechmann, M., Polaschegg, C., Herrmann, N., Goldbeck, I., Dittmann, K., and Wienands, J. (2007) SLP-65 signal trans-

- duction requires Src homology 2 domain-mediated membrane anchoring and a kinase-independent adaptor function of Syk. *J. Biol. Chem.* **282**, 29059–29066
24. Kurosaki, T., Maeda, A., Ishiai, M., Hashimoto, A., Inabe, K., and Takata, M. (2000) Regulation of the phospholipase C-gamma2 pathway in B cells. *Immunol. Rev.* **176**, 19–29
  25. Ishiai, M., Kurosaki, M., Pappu, R., Okawa, K., Ronko, I., Fu, C., Shibata, M., Iwamatsu, A., Chan, A. C., and Kurosaki, T. (1999) BLNK required for coupling Syk to PLC gamma 2 and Rac1-JNK in B cells. *Immunity* **10**, 117–125
  26. Oh-hora, M., and Rao, A. (2008) Calcium signaling in lymphocytes. *Curr. Opin. Immunol.* **20**, 250–258
  27. Hashimoto, A., Okada, H., Jiang, A., Kurosaki, M., Greenberg, S., Clark, E. A., and Kurosaki, T. (1998) Involvement of guanosine triphosphatases and phospholipase C-gamma2 in extracellular signal-regulated kinase, c-Jun NH2-terminal kinase, and p38 mitogen-activated protein kinase activation by the B cell antigen receptor. *J. Exp. Med.* **188**, 1287–1295
  28. Foletta, V. C., Segal, D. H., and Cohen, D. R. (1998) Transcriptional regulation in the immune system: all roads lead to AP-1. *J. Leukoc. Biol.* **63**, 139–152
  29. Grabbe, A., and Wienands, J. (2006) Human SLP-65 isoforms contribute differently to activation and apoptosis of B lymphocytes. *Blood* **108**, 3761–3768
  30. Di Bartolo, V., Montagne, B., Salek, M., Jungwirth, B., Carrette, F., Fourtane, J., Sol-Foulon, N., Michel, F., Schwartz, O., Lehmann, W. D., and Acuto, O. (2007) A novel pathway down-modulating T cell activation involves HPK-1-dependent recruitment of 14–3–3 proteins on SLP-76. *J. Exp. Med.* **204**, 681–691
  31. Pinkse, M. W., Uitto, P. M., Hilhorst, M. J., Ooms, B., and Heck, A. J. (2004) Selective isolation at the femtomole level of phosphopeptides from proteolytic digests using 2D-NanoLC-ESI-MS/MS and titanium oxide precolumns. *Anal. Chem.* **76**, 3935–3943
  32. Larsen, M. R., Thingholm, T. E., Jensen, O. N., Roepstorff, P., and Jørgensen, T. J. (2005) Highly selective enrichment of phosphorylated peptides from peptide mixtures using titanium dioxide microcolumns. *Mol. Cell. Proteomics* **4**, 873–886
  33. Ong, S. E., Blagoev, B., Kratchmarova, I., Kristensen, D. B., Steen, H., Pandey, A., and Mann, M. (2002) Stable isotope labeling by amino acids in cell culture, SILAC, as a simple and accurate approach to expression proteomics. *Mol. Cell. Proteomics* **1**, 376–386
  34. Olsen, J. V., Blagoev, B., Gnäd, F., Macek, B., Kumar, C., Mortensen, P., and Mann, M. (2006) Global, in vivo, and site-specific phosphorylation dynamics in signaling networks. *Cell* **127**, 635–648
  35. Buerstedde, J. M., and Takeda, S. (1991) Increased ratio of targeted to random integration after transfection of chicken B cell lines. *Cell* **67**, 179–188
  36. Stork, B., Engelke, M., Frey, J., Horejsi, V., Hamm-Baarke, A., Schraven, B., Kurosaki, T., and Wienands, J. (2004) Grb2 and the non-T cell activation linker NTAL constitute a Ca(2+)-regulating signal circuit in B lymphocytes. *Immunity* **21**, 681–691
  37. Boeri Erba, E., Matthiesen, R., Bunkenborg, J., Schulze, W. X., Di Stefano, P., Cabodi, S., Tarone, G., Defilippi, P., and Jensen, O. N. (2007) Quantitation of multisite EGF receptor phosphorylation using mass spectrometry and a novel normalization approach. *J. Proteome Res.* **6**, 2768–2785
  38. Berberich, I., Shu, G. L., and Clark, E. A. (1994) Cross-linking CD40 on B cells rapidly activates nuclear factor-kappa B. *J. Immunol.* **153**, 4357–4366
  39. Brummer, T., Shaw, P. E., Reth, M., and Misawa, Y. (2002) Inducible gene deletion reveals different roles for B-Raf and Raf-1 in B-cell antigen receptor signaling. *EMBO J.* **21**, 5611–5622
  40. Winding, P., and Berchtold, M. W. (2001) The chicken B cell line DT40: a novel tool for gene disruption experiments. *J. Immunol. Methods* **249**, 1–16
  41. Schroeder, M. J., Shabanowitz, J., Schwartz, J. C., Hunt, D. F., and Coon, J. J. (2004) A neutral loss activation method for improved phosphopeptide sequence analysis by quadruple ion trap mass spectrometry. *Anal. Chem.* **76**, 3590–3598
  42. Blagoev, B., Ong, S. E., Kratchmarova, I., and Mann, M. (2004) Temporal analysis of phosphotyrosine-dependent signaling networks by quantitative proteomics. *Nat. Biotechnol.* **22**, 1139–1145
  43. Schulze, W. X., and Mann, M. (2004) A novel proteomic screen for peptide-protein interactions. *J. Biol. Chem.* **279**, 10756–10764
  44. Zhang, R., Sioma, C. S., Wang, S., and Regnier, F. E. (2001) Fractionation of isotopically labeled peptides in quantitative proteomics. *Anal. Chem.* **73**, 5142–5149
  45. Shinohara, H., and Kurosaki, T. (2006) Genetic analysis of B cell signaling. *Subcell. Biochem.* **40**, 145–187
  46. Baba, Y., Hashimoto, S., Matsushita, M., Watanabe, D., Kishimoto, T., Kurosaki, T., and Tsukada, S. (2001) BLNK mediates Syk-dependent Btk activation. *Proc. Natl. Acad. Sci. U.S.A.* **98**, 2582–2586
  47. Ohno, Y., Yagi, H., Nakamura, M., Masuko, K., Hashimoto, Y., and Masuko, T. (2008) Cell-death-inducing monoclonal antibodies raised against DT40 tumor cells: identification of chicken transferrin receptor as a novel cell-death receptor. *Cancer Sci.* **99**, 894–900
  48. Lahti, J. M. (1999) Use of gene knockouts in cultured cells to study apoptosis. *Methods* **17**, 305–312
  49. Reth, M., and Wienands, J. (1997) Initiation and processing of signals from the B cell antigen receptor. *Annu. Rev. Immunol.* **15**, 453–479
  50. Jaquet, K., Thieleczek, R., and Heilmeyer, L. M., Jr. (1995) Pattern formation on cardiac troponin I by consecutive phosphorylation and dephosphorylation. *Eur. J. Biochem.* **231**, 486–490
  51. Engels, N., Wollscheid, B., and Wienands, J. (2001) Association of SLP-65/BLNK with the B cell antigen receptor through a non-ITAM tyrosine of Ig-alpha. *Eur. J. Immunol.* **31**, 2126–2134
  52. Ledbetter, J. A., Rabinovitch, P. S., June, C. H., Song, C. W., Clark, E. A., and Uckun, F. M. (1988) Antigen-independent regulation of cytoplasmic calcium in B cells with a 12-kDa B-cell growth factor and anti-CD19. *Proc. Natl. Acad. Sci. U.S.A.* **85**, 1897–1901
  53. de Rie, M. A., Schumacher, T. N., van Schijndel, G. M., van Lier, R. A., and Miedema, F. (1989) Regulatory role of CD19 molecules in B-cell activation and differentiation. *Cell. Immunol.* **118**, 368–381
  54. Nitschke, L., Carsetti, R., Ocker, B., Köhler, G., and Lamers, M. C. (1997) CD22 is a negative regulator of B-cell receptor signaling. *Curr. Biol.* **7**, 133–143
  55. Chen, J., McLean, P. A., Neel, B. G., Okunade, G., Shull, G. E., and Wortis, H. H. (2004) CD22 attenuates calcium signaling by potentiating plasma membrane calcium-ATPase activity. *Nat. Immunol.* **5**, 651–657